Received: 31 October 2019 | Revised: 4 March 2020 | Accepted: 8 March 2020

DOI: 10.1002/aoc.5704

FULL PAPER

Applied Organometallic Chemistry WILEY

Zirconium@guanine@MCM-41 nanoparticles: An efficient heterogeneous mesoporous nanocatalyst for one-pot, multi-component tandem Knoevenagel condensation–Michael addition–cyclization Reactions

Mohsen Nikoorazm | **Masoud Mohammadi** | **Maryam Khanmoradi**

Department of Chemistry, Faculty of Science, Ilam University, Ilam, Iran

Correspondence
Mohsen Nikoorazm, Department of Chemistry, Faculty of Science, Ilam University, Ilam, Iran.
Email: e_nikoorazm@yahoo.com

Funding information
Ilam University; Iran National Science Foundation

MCM-41-supported nanoscale guanine bonded with Zr (IV) was prepared using sol–gel method and characterized by FT-IR, Raman, XRD, BET, TGA, EDX, ICP, AAS, X-Ray mapping, SEM and TEM techniques. This compound was employed as an efficient, chemoselectivity and green heterogeneous catalyst in order to prepare a series of benzo[a]benzo[6,7]chromeno[2,3-c] phenazine and spiro[benzo[a]benzo[6,7]chromeno[2,3-c] phenazine] derivatives by one-pot, four-component domino reaction from the 2-hydroxy-1,-4-naphthoquinone, benzene-1,2-diamines, 2-hydroxy-1,4-naphthoquinone and carbonyl compounds in PEG, at 100 °C and, also, Bis (pyrazolyl) methane derivatives using aldehydes and 3-Methyl-1-phenyl-5-pyrazolone in ethanol under reflux condition. Results indicated that all products were synthesized in short reaction times and high yields in the ranges 78–99%. The Zr-guanine-MCM-41 can be recycled four runs without any significant loss of its catalytic activity. In addition, the stability of the catalyst was confirmed by metal leaching, heterogeneity tests, SEM and FT-IR techniques.

KEYWORDS

benzo[a]benzo[6,7]chromeno[2,3-c]phenazines, Bis (pyrazolyl)methanes, Spiro[benzo[a] benzo[6,7]chromeno[2,3-c] phenazine], Tandem Knoevenagel condensation–Michael addition–cyclization, Zr-guanine-MCM-41

1 | INTRODUCTION

Discovery of new chemical reactions which are able to produce useful chemical products has been the subject of much interest.[1–3] Traditional methods are unsustainable to perform chemical synthesis from economic and environmental points of view.[4,5] Multi-component reactions (MCRs) have come out as a powerful tool in modern synthetic organic chemistry and provide a solution to overcome the mentioned disadvantages.[4,6–9] In this respect, it is significant to note that the benefits of multi-component reactions (MCRs) in combinatorial chemistry are highly regarded in nature; as they are essential to life and minimize the waste production, time, cost and labor.[10,11] These reactions have become a strong synthetic methodology for the rapid preparation of small-molecule libraries that reduce the number of synthetic steps and can be obtained in one pot with much fewer steps.[8,12–14] The major advantages of multicomponent reactions are one-pot synthesis, high atom economy and time-saving without isolation of intermediates or generating by-products.[14–19] In particular, Phenazines and chromenes have attracted increasing attention in drug

discovery and medicinal chemistry which can be synthesized by a one-pot two-steps procedure.[8,18–20] These compounds have been reported as biological active species which involve anticancer, antifungal, antiplasmodial, antimalarial, antibacterial, cancer chemopreventive, antiparasitic and antichagasagen activities.[19] Among the wide range of N-containing heterocyclic compounds, the pyrazolones and bis-pyrazolones were paid much attention for their various biological activities, such as antitumor,[21] anti-inflammatory,[22] antifilarial agents,[23] dyes,[24] pesticides,[14] selective COX-2 inhibitory,[25] antibacterial[23] and fungicides.[15] Moreover, these compounds were used as extracting agents for some metal ions in analytical chemistry[26] and ligands in coordination chemistry.[27]

The development of new plans for catalytic stability in reaction medium that minimizes the cost and toxicity can result in important environmental and economic interests.[4,28–32] The regular cylindrical arrangement structure, heterogeneity and reusability of MCM-41 (Mobil Composition of Matter No. 41) mesoporous silica make it a great candidate as a heterogeneous solid catalyst, which can be functionalized by reacting with organosilanes groups and the substitution of metal complexes inside the mesoporous silica framework.[33–35] MCM-41 with a hexagonal arrangement and diameter of 2 nm to 10 nm and, also, owing to a uniform open form structure, low cytotoxicity, low cost, simple synthesis, biocompatibility, excellent stability, uniform catalytic sites and large pore volume and surface area can act as an excellent support which is able to increase the catalytic activity.[36,37] Transitional metal complexes have been greatly studied in the catalyst field due to the solubility properties of transition metal complexes in the aqueous phase and also in drug discovery in accordance to their cytotoxic, antimicrobial and antitumor properties.[9,11,32,38] There is not much information on zirconium (IV) complexes in the synthesis of benzo[a]benzo[6,7]chromeno[2,3-c]phenazine derivatives. Therefore, in this work, the guanine complex of zirconium ions supported on modified MCM-41 nanoparticles has been synthesized and characterized by FT-IR, Raman, XRD, BET, TGA, EDX, ICP, AAS, X-Ray mapping, SEM and TEM techniques. According to the structure of guanine, in several models of metal complexes, the metal ions bind to the guanine ring through carbonyl oxygen O (6) and/or imidazolyl nitrogen, N (7) and/or N (1) position of guanine).[38] Afterwards, they are used as an efficient catalyst for the clean and facile one-pot domino synthesis of spiro[benzo[*a*]benzo[6,7]chromeno[2,3-*c*]phenazine], benzo[*a*]benzo[6,7]chromeno[2,3-*c*]phenazine and bis (pyrazolyl)methane derivatives via the Knoevenagel condensation–Michael addition–cyclization reactions of 2-hydroxy-1,4-naphthoquinone (lawsone), benzene-1,2-diamine and carbonyl compounds (aldehydes and ninhydrin and isatin as cyclic ketones) and the Knoevenagel condensation–Michael addition reactions of 3-Methyl-1-phenyl-5-pyrazolone with aryl aldehydes. The main advantages of this synthesis include simple workup, reusability of the catalyst, easy recovery and fewer reaction steps without the intermediates separation.

2 | EXPERIMENTAL SECTION

2.1 | Materials

Tetraethylorthosilicate (TEOS, 98%), cationic surfactant cetyltrimethylammonium bromide (CTAB, 98%), guanine (2-amino-1*H*-purin-6(9*H*)-one), Zr (IV) oxide chloride ($ZrO\ Cl_2.8H_2O$), aromatic aldehydes, cyclic ketones, 2-hydroxy-1,4-naphthoquinone, benzene-1,2-diamines, 3-chloropropyl-triethoxysilane, solvents and other reagents, that were employed in this work, were purchased from Aldrich, Merck or Fluka chemical companies and used as received.

2.2 | Characterization techniques

Powder X-ray diffraction (PXRD) of Zr-guanine-MCM-41 catalyst was recorded using a Holland Philips diffractometer (Cu Kα, radiation at 40 kV and 30 mA). The thermogravimetric analysis (TGA) curve was obtained between 30 and 900 °C in air at a heating rate of 10 °C min^{-1} using Shimadzu DTG-60 automatic thermal analyzer. The infrared spectra (IR) of the samples were recorded in KBr disks using a NICOLET impact 410 spectrometer. The particle size and morphology were investigated by a JEOLJEM-2010 scanning electron microscopy (SEM), on an accelerating voltage of 200 kV. The transmission electron microscopy (TEM) images were recorded by a Philips CM10 microscope with operating voltage at 200 kV. The products' component measurement was carried out by the energy dispersive spectroscopy (EDX) using a Tacnai TF20 high-resolution transmission electron microscope. The Raman spectrum of the catalyst was taken with a Jobin Yvon U1000 spectrometer. The content of Zr was measured by inductively coupled plasma-optical emission spectrometry (ICP-OES) and AAS analysis in a NovAA 400p Analyticaljena-Germany device.

2.3 | Synthesis of MCM-41 modified with (3-chloropropyl)-triethoxysilane

The mesoporous silica MCM-41 nanoparticles were prepared by the coprecipitation technique as it was previously reported.[39] In order to produce the pure siliceous MCM-41, cetyltrimethylammonium bromide (CTAB) (1 g), which can be regarded as a cationic surfactant, was added into a basic aqueous solution (3.5 ml of NaOH (2 M) in 480 ml of deionized water. The chemicals were stirred vigorously and heated up to 80 °C until the solution became uniform and, then, 5 ml tetraethylorthosilicate (TEOS) was added dropwise to this solution. Afterwards, the resulting solution was refluxed for another 2 hr. After the reaction time, the heating was stopped and the suspension was cooled down to room temperature. Then, the solid particles were collected by filtration, washed with deionized water and dried overnight in an oven at 70 °C. Ultimately, the dried precipitate was calcined from room temperature to 550 °C for 5 hr with the heating rate of 2 °C/min. Afterwards, in order to synthesize CPTMS@MCM-41 in accordance to the previously reported procedure,[40] a mixture of MCM-41 and 3-chloropropyl-triethoxysilane (nPrCl), in a molar ratio 1:1, was dissolved in *n*-hexane and refluxed for 20 hr under a nitrogen atmosphere. After the reaction time, the precipitate was separated by simple filtration, subsequently washed with *n*-hexane and, finally, dried at 50 °C.

2.4 | Synthesis of guanine functionalized MCM-41 mesoporous material (guanine-MCM-41)

Firstly, 0.5 g of CPTMS@MCM-41 and 2-amino-1*H*-purin-6(9*H*)-one (guanine) (1.2 mmol, 0.181 g), in 20 ml toluene were refluxed under nitrogen atmosphere for 24 hr. The obtained white precipitate was filtered and washed with ethanol and, finally, the solvent was removed under vacuum.

2.5 | Synthesis of heterogeneous catalyst (Zr-guanine-MCM-41)

In this step, guanine-MCM-41 (0.25 g) was mixed with Zr (IV) oxide chloride (ZrO $Cl_2.8H_2O$) (0.5 mmol, 0.161 g) in ethanol (20 ml) and refluxed for 20 hr. After the completion of the reaction, the chemicals were collected by filtration, intensively washed by ethanol and, finally, dried at 50 °C in order to give the Zr-guanine-MCM-41 complex (Scheme 1).

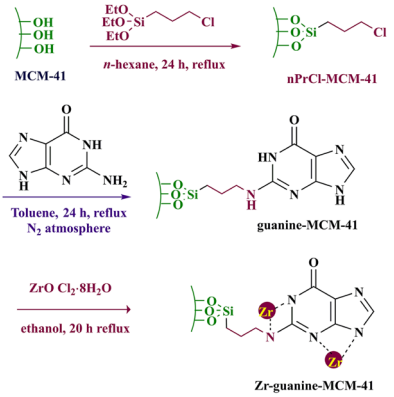

SCHEME 1 Synthesis of Zr-guanine-*MCM*-41 nanostructure

2.6 | General procedure for the synthesis of spiro[benzo[a]benzo[6,7]chromeno[2,3-c]phenazine] and benzo[a]benzo[6,7]chromeno[2,3-c]phenazine derivatives

This One-pot, four-component, two-steps reaction was applied according to the below procedure: first, the 2-hydroxy-1,4-naphthoquinone (1 mmol), benzene-1,-2-diamines (1 mmol) and Zr- guanine-MCM-41 (0.30 mol%) were placed into a round bottom flask containing 3 ml PEG-400 and, then, the obtained chemicals were stirred and heated at 100 °C until the compound A is formed (10 min) (scheme 3). In the second step, the reaction was followed by the addition of 2-hydroxy-1,-4-naphthoquinone (1 mmol) and carbonyl compounds (1 mmol) (aldehyde and cyclic ketones (ninhydrin and isatin)) and, then, the resultant was heated further under the same conditions for the times exhibited in Table 3. The progress of the reaction was determined by TLC. After the completion of the reaction, the resulting mixture was decanted in water and ethyl acetate. The catalyst was filtered, and the product was collected by evaporation of ethyl acetate. For more purification, recrystallization of the generated solid has been applied from hot ethanol to the obtained pure product.

2.7 | General pathway for the synthesis of 4,4′-(arylmethylene)-bis-(3-methyl-1-phenyl-1H-pyrazol-5-ols)

A mixture of aldehyde (1 mmol), 3-Methyl-1-phenyl-5-pyrazolone (2 mmol) and Zr-gu-MCM-41 (0.25 mol%) was dissolved in 3 ml of EtOH. Afterwards, the flask was sealed and stirred at reflux conditions (80 °C). The progress of the reaction was monitored by TLC (n-hexane/ethyl acetate: 4/1). After completion of the reaction, (the mixture was cooled down to room temperature,

filtered and, then, washed with hot EtOH to separate the catalyst from other materials (the reaction mixture was soluble in hot EtOH and the solid catalyst was insoluble). Finally, the solvent removal was carried out and for further purification to yield pure products, the crude product was recrystallized by ethanol.

3 | RESULTS AND DISCUSSION

3.1 | Catalyst preparation

In this research, Zr-guanine complex anchored onto the MCM-41 mesoporous support (Zr-guanine-MCM-41) has been introduced as a reusable zirconium based nanocatalyst. Initially, the MCM-41 nanoparticles have been easily prepared in water by the coprecipitation technique. Afterwards, it was modified using the immobilization of nPrCl and, then, 2-amino-1H-purin-6(9H)-one (guanine) supported into MCM-41 mesoporous (Zr-guanine-MCM-41as a green ligand was grafted onto the modified MCM-41 mesoporous support in green conditions. Finally, the Zr-guanine complex was synthesized by the reaction of guanine-MCM-41with Zr (IV) oxide chloride (Scheme 1).

3.2 | Catalyst characterizations

The as-prepared Zr-guanine-MCM-41catalyst was characterized using FT-IR, Raman, XRD, BET, TGA, EDX, ICP, AAS, X-Ray mapping, SEM and TEM techniques.

The selected vibrational frequencies for MCM-41, nPrCl-MCM-41, guanine-MCM-41 ligand and Zr-guanine-MCM-41 complex are prepared by FT-IR spectroscopy as presented in Figure 1. The observation peaks at 1059, 962 cm^{-1} and 452 cm^{-1} are corresponding to the asymmetric stretching and the symmetric stretching and bending Si-O–Si vibrations respectively indicate the synthesis of MCM-41 (Figure 1a). The FT-IR spectrum of the modified MCM-41 (nPrCl-MCM-41) exhibits a broad band at 3442 cm^{-1} duo to the hydrogen-bonding silanol groups and the adsorbed water. Figure 1b confirmed that the C–H stretching of CH_2 vibrations was appeared at about 2924 cm^{-1}. In Figure 1c, the absence of this characteristic band of C − H vibration and the presence of

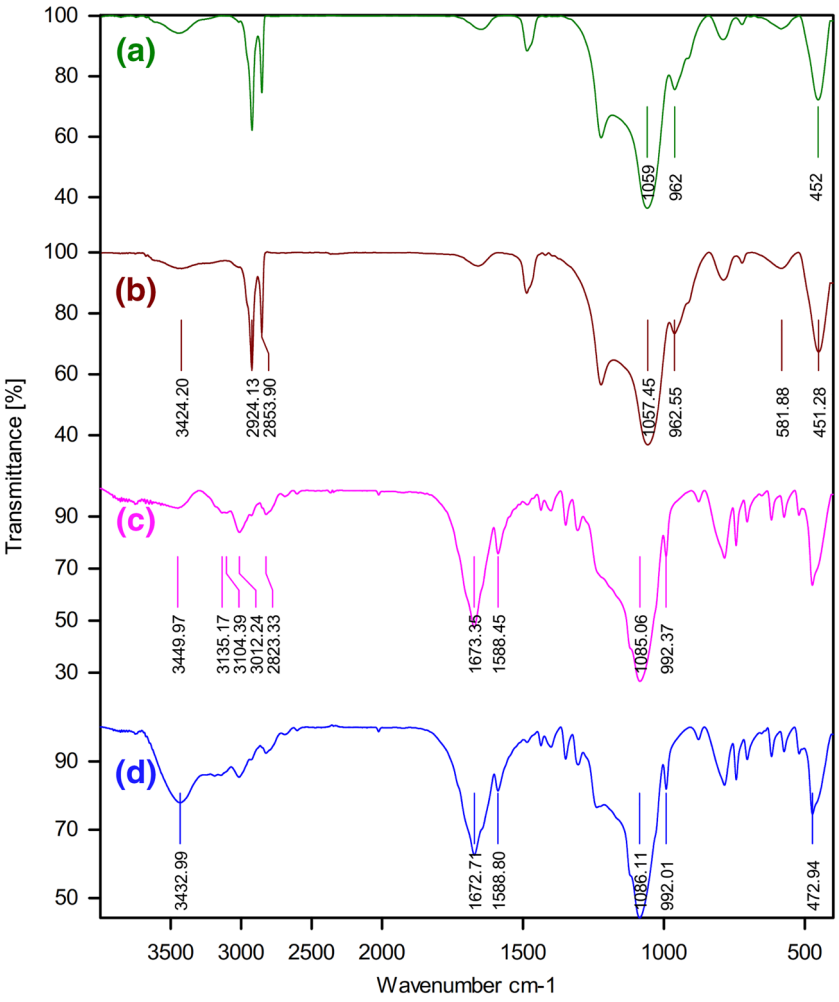

FIGURE 1 The FT-IR spectra for pure MCM-41(a), nPrCl-MCM-41(b), guanine-MCM-41 (c) and Zr-guanine-MCM-41 (d)

signals at 1588 cm^{-1} (C=O) and 1673 cm^{-1} (C=N) emphasize the presence of carboxyl and imine functional groups of guanine (2-amino-1H-purin-6(9H)-one) ring and, also, the successful removal of CTAB. The FT-IR spectrum of the metal complex in Figure 1d indicates the coordination of the metal to the guanine-MCM-41. The Zr-guanine-MCM-41 complex showed the band at 3432 cm^{-1} while, in guanine-MCM-41, the mentioned band appeared at 3449 cm^{-1}. This chemical shift is attributed to the formation of zirconium complex.

Raman spectrum of Zr-guanine-MCM-41 is presented in Figure 9. The band at around 879 cm^{-1} which is the characteristic for the fourfold coordinated zirconium in silicate structures also appears in the infrared spectrum of Zr-guanine-MCM-41 at 877 cm^{-1} (Figure 1d) but not in the IR (Figure 1c) or raman spectrum of MCM-41 sample.[44] There is a couple of wide and medium peaks, indicating the stretching vibration of the aliphatic carbon chains between 600 to 1300 cm^{-1}, which comes from the moieties of 3-amino propyl three ethoxy silane (3-APTES) on the surface of MCM-41. Besides, the appearance peak at around 560 cm^{-1} that is attributed to (Si-O-Si) shows that 3-APTES has been successfully functionalized on the MCM-41. The medium bending vibration peak of $-CH_2$ function is from 1400–1470 cm^{-1}.[44] These observations confirm the functionalization of the catalyst.

Figure 3 shows the low angle powder X-ray diffraction patterns of the Zr-guanine-MCM-41. As reported in our previous works,[45–48] MCM-41 phase was identified from the XRD patterns by the three characteristic peaks related to the strong (100), smaller (110) and (200) reflections which confirm the hexagonal pore arrangement of MCM-41. According to Figure 2,3, in the XRD patterns of the Zr-guanine-MCM-41, there were no well-resolved peaks corresponding to d_{100}, d_{110} and, also, the decrease in the intensity of the peak at d_{100} which can be regarded as a strong evidence reveals that the well-grafting of zirconium complex into MCM-41 channels was occurred.

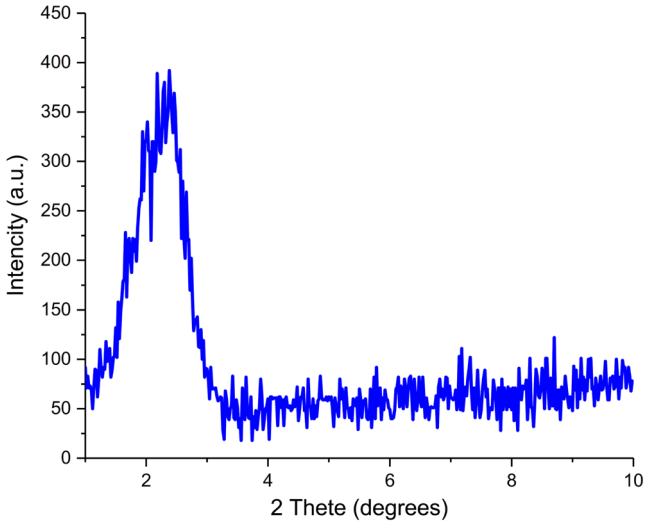

FIGURE 3 XRD pattern of Zr-guanine-MCM-41

For further study, N_2 adsorption–desorption of Zr-guanine-MCM-41 was performed as the obtained information is shown in Table 1. The BET curves that are shown in Figure 4 indicate that the typical Type IV isotherms are related to the characteristics of mesoporous materials with highly uniform size distributions. According to the Table 1, we can observe that BET surface area, pore volume and pore diameter of Zr-guanine-MCM-41 are less than the MCM-41 calculated in the previous works.[49] These observations indicate that the Zr complex has been successfully immobilized inside the pore channels. The values of wall thickness of Zr-

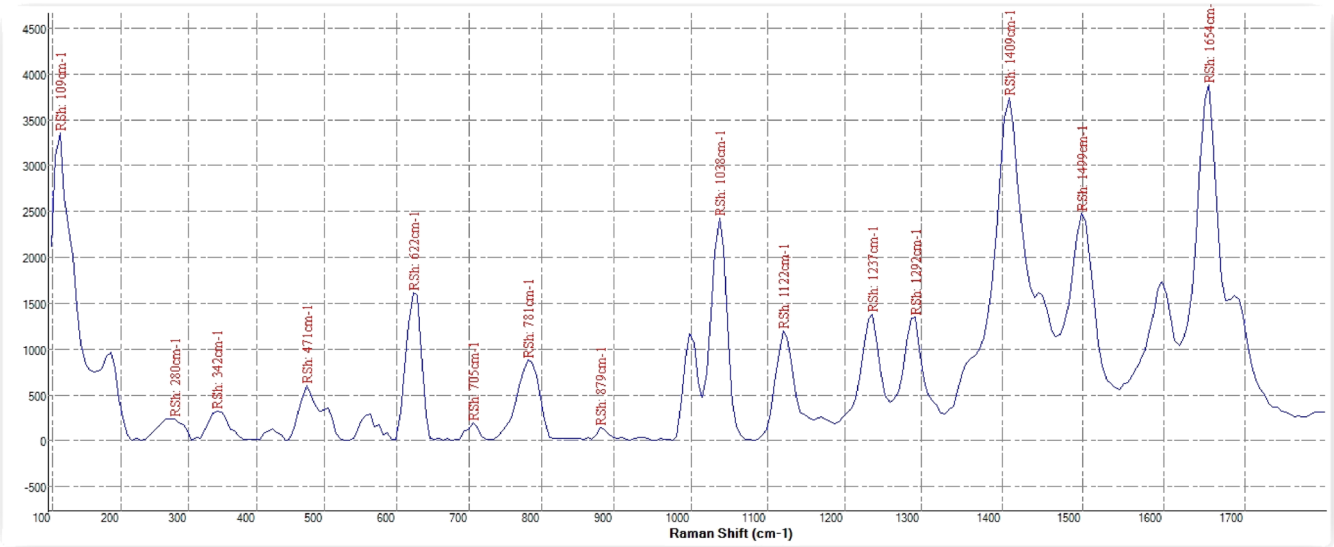

FIGURE 2 Raman spectra of Zr-guanine-MCM-41

TABLE 1 Surface properties of Zr-guanine-MCM-41

Sample	S_{BET} (m^2/g)	Pore diam. (nm)	Pore vol. (cm^3/g)	Wall thickness
MCM-41 [46]	1372.275	2.45	1.521	0.5
Zr-guanine-MCM-41	332.66	1.29	0.467	1.11

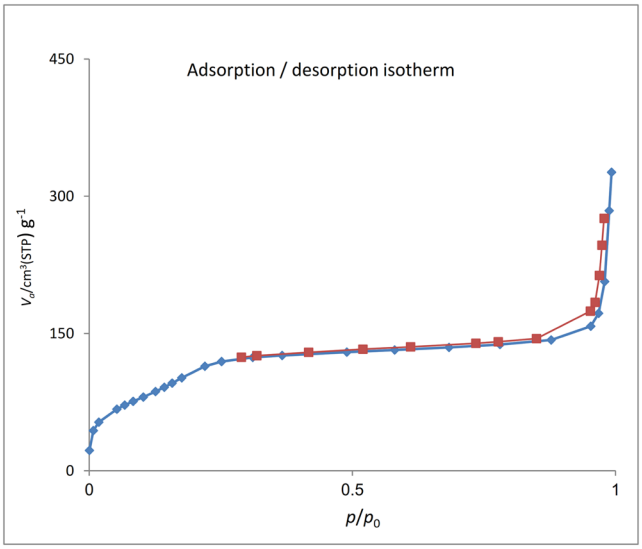

FIGURE 4 Adsorption/Desorption isotherm Zr-guanine-MCM-41

guanine-MCM-41, calculated by the below equation, has been illustrated in Table 1.

$$\text{Wall thickness}: 2d_{100}/\left(\sqrt{3}\right) - D_{BJH}$$

The thermal stability of Zr-guanine-MCM-41 was studied by thermal gravimetric analysis (TGA) (Figure 5). Zr-guanine-MCM-41 exhibits a one-step weight loss below 100 °C (~4%) due to the loss of the adsorbed water and the organic solvent. But, at above 100 °C, two other weight losses are also observed. The weight loss was appeared in the temperature range of 200–350 °C (10.42%) which is related to the decomposition of organic moieties. Moreover, the major weight loss between 400–650 °C is chiefly associated with the decomposition of silanol groups and the organically modified framework.[5,9,50]

Energy dispersive X-ray spectroscopy (EDX) analysis of Zr-guanine-MCM-41 is carried out to indicate the adsorption of zirconium on the surface of MCM-41 (Figure 6). In EDX image, the peaks associated with Zr (1.84%), Si (24.48%), O (50.14%), C (6.56%) and N (16.98%) can be observed. As expected, the amount of nitrogen is a quarter than the amount of zirconium, which is in good agreement with the structure of Zr-guanine-MCM-41 in Scheme 1.

X-Ray map analysis was studied in order to explore the dispersion of all elements of the catalyst structure. The results shown in Figure 7 illustrate the good dispersion of all the elements on the surface of Zr-guanine-MCM-41. In this sense, the results clearly confirmed the results of EDS analysis.

Also, the amount of zirconium ions which was obtained by ICP analysis was found to be 1.051×10^{-3} mol g^{-1} which is in good agreement with AAS analysis illustrating 1.048×10^{-3} mol $g^{-1}$of zirconium in the Zr-guanine-MCM-41.

The Images on the scanning electron microscopy (SEM) in Figure 8 showed the spherical particle morphology with small and uniform nanoparticles and without impurities for Zr-guanine-MCM-41 sample.

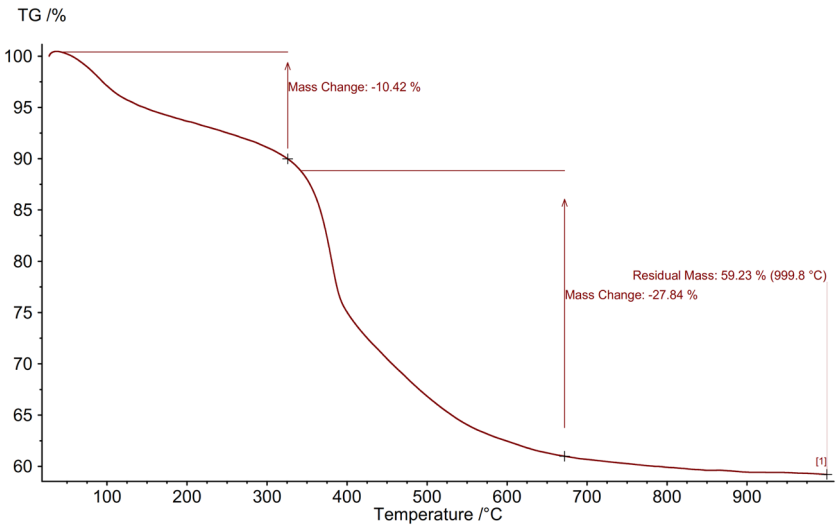

FIGURE 5 TGA thermograms of Zr-guanine-MCM-41

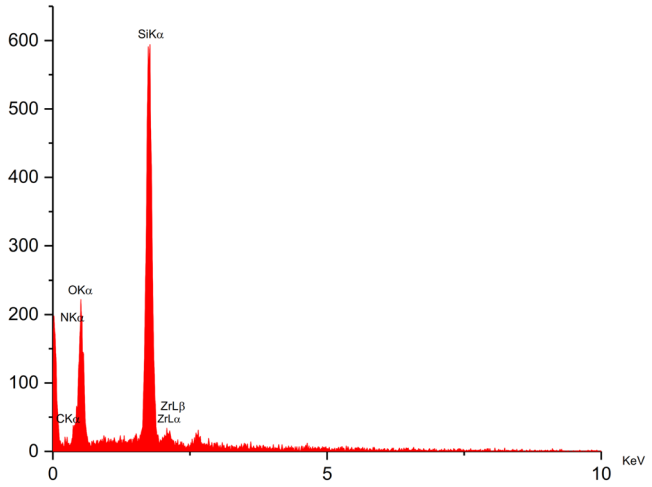

FIGURE 6 EDX spectrum of Zr-guanine-MCM-41

TEM micrographs of Zr-guanine-MCM-41 sample (Figure 9) confirm the well-ordered lattice of the hexagonal channels in the prepared mesoporous functionalized catalyst. In addition, TEM images show a clear hexagonal arrangement of pores with uniform size.

3.3 | Application of heterogeneous catalysts

The present study investigates an efficient, facile, and environmentally friendly procedure for one-pot tandem Knoevenagel condensation–Michael addition–cyclization reactions in order to synthesize benzo[*a*]benzo[6,7]chromeno[2,3-*c*]phenazines,spiro[benzo[*a*]benzo[6,7] chromeno [2,3-*c*] phenazine], and Bis (pyrazolyl)methane derivatives using Zr-guanine-MCM-41 as a heterogeneous and efficient catalyst.

Initially, the catalytic properties of Zr-guanine-MCM-41 were examined in the Synthesis of benzo[*a*]benzo[6,7] chromeno[2,3-*c*]phenazines,spiro[benzo[*a*]benzo[6,7] chromeno [2,3-*c*] phe-nazine].

In order to establish the feasibility of this protocol and find the optimal conditions for the synthesis of benzo[*a*]benzo[6,7]chromeno[2,3-*c*]phenazine and spiro[benzo[*a*]benzo[6,7]chromeno[2,3-*c*] phenazine] derivatives, we explored the reaction of 2-hydroxy-1,-4-naphthoquinone, benzene-1,2-diamines, and 4-chlorobenzaldehyde as the model reaction. We also aimed at investigating the effect of different reaction parameters such as the amount of the catalyst, nature of solvents and reaction temperature on the rate of the chemical reaction and the yield of products (Scheme 2).

In order to establish the appropriate amount of the catalyst, various loadings of the catalyst were studied (Table 2, entries 5–12) and, consequently, 30 mol% of the catalyst on the basis of Zr was found to be more effective in terms of the best yield (Table 2, entry 11). In an attempt to find the best solvent, the reaction was explored using different solvents such as PEG-400, DMF, EtOH and H_2O (Table 2, entries 13–20). We found out that the reaction in PEG-400 as the solvent was achieved with 90 present yield of the desired product in 2 hr

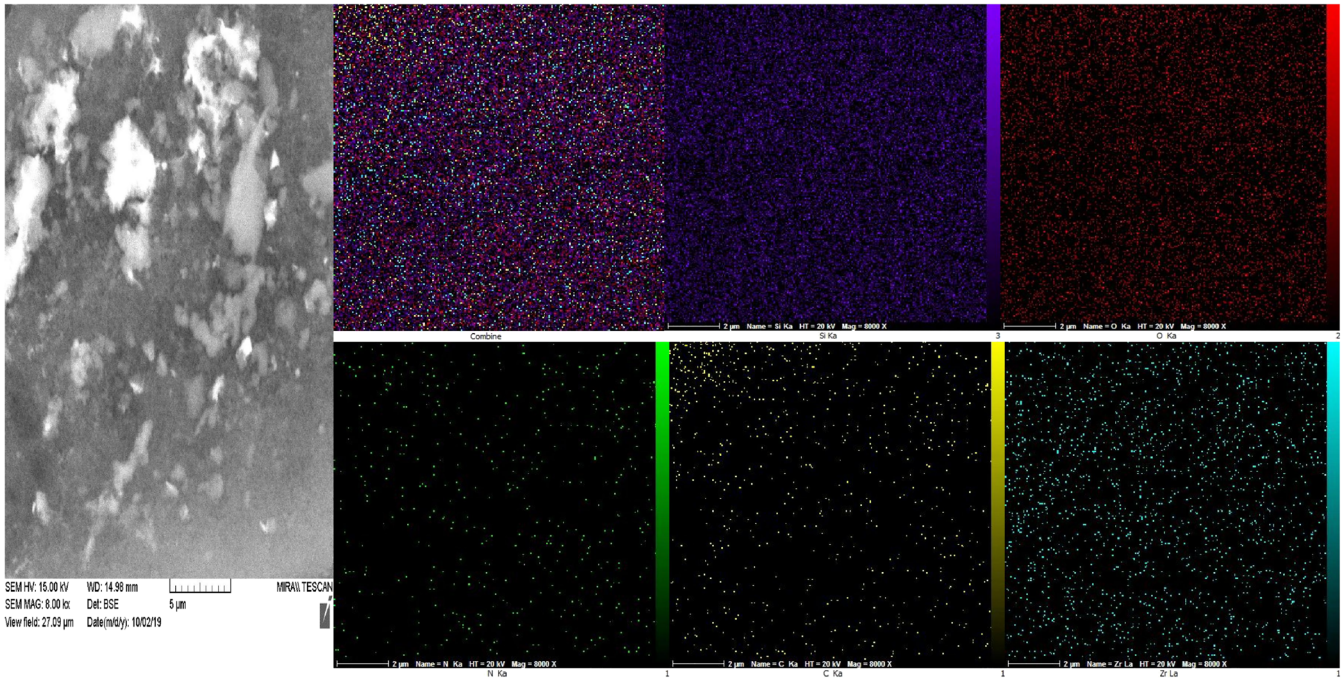

FIGURE 7 Elemental mapping of (a) zirconium, (b) oxygen, (c) silica, (d) carbon and (e) nitrogen for Zr-guanine-MCM-41

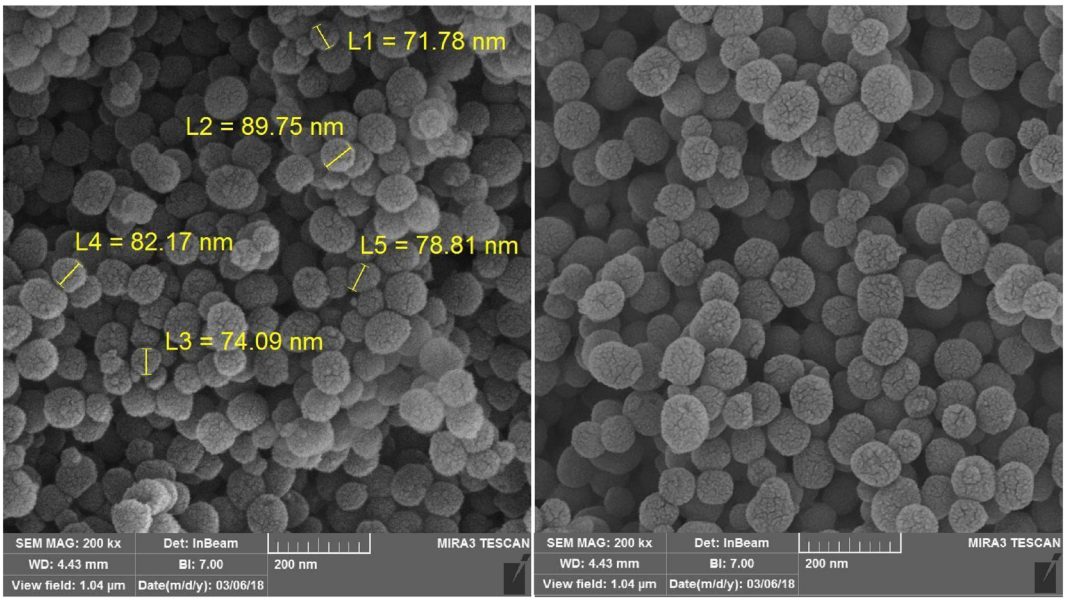

FIGURE 8 SEM images of Zr-guanine-MCM-41

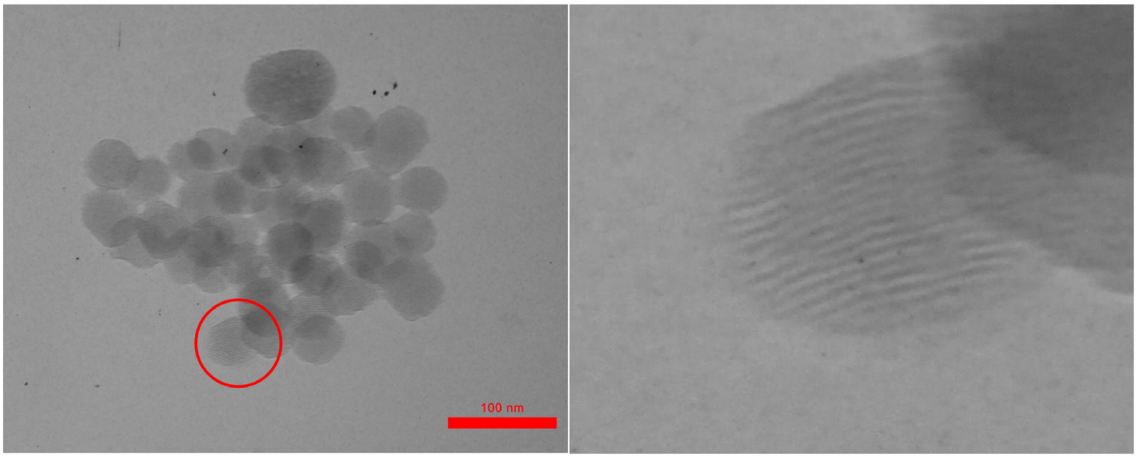

FIGURE 9 TEM images of Zr-guanine-MCM-41

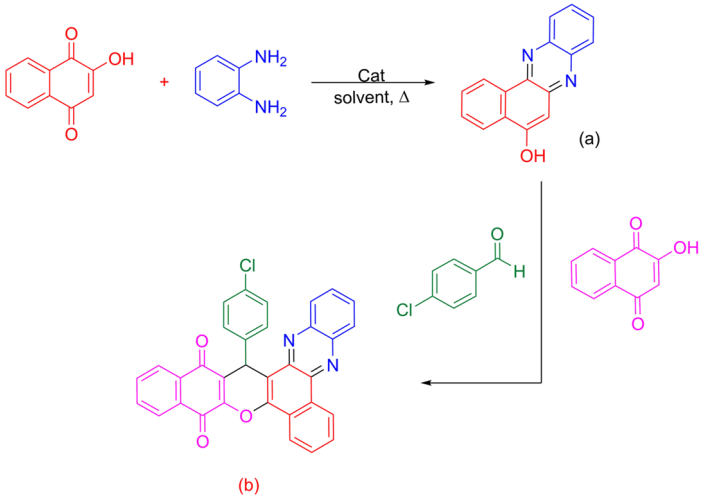

SCHEME 2 Optimization of reaction conditions for the preparation of 17-(4-chlorophenyl)-11H benzo[a]benzo[6,7] chromeno[2,3-c]phenazine-11,16(17H)-dione

TABLE 2 Optimization of reaction conditions for the preparation of 17-(4-chlorophenyl)-11H benzo[a]benzo[6,7]chromeno[2,3-c] phenazine-11,16(17H)-dione

Entry	Catalyst	Amount of catalyst (mol%)	Solvent	Temperature (°C)	Time (h)	Yield (%)[a]
1	ZrO Cl_2.8H_2O	0.30	PEG-400	100	2	27
2	Guanine	0.30	PEG-400	100	2	Trace
3	MCM-41	25 mg	PEG-400	100	2	NR[b]
4	Zr- MCM-41	25 mg	PEG-400	100	4	34
5	guanine-MCM-41	25 mg	PEG-400	100	2	Trace
6	-	-	PEG-400	100	48	NR[b]
7	Zr-guanine-MCM-41	0.05	PEG-400	100	2	35
8	Zr-guanine-MCM-41	0.1	PEG-400	100	2	47
9	Zr-guanine-MCM-41	0.15	PEG-400	100	2	58
10	Zr-guanine-MCM-41	0.20	PEG-400	100	2	67
11	Zr-guanine-MCM-41	0.25	PEG-400	100	2	83
12	Zr-guanine-MCM-41	0.30	PEG-400	100	2	90
13	Zr-guanine-MCM-41	0.35	PEG-400	100	2	90
14	Zr-guanine-MCM-41	0.30	EtOH	70	5	63
15	Zr-guanine-MCM-41	0.30	EtOH	reflux	5	76
16	Zr-guanine-MCM-41	0.30	H_2O	reflux	2	b
17	Zr-guanine-MCM-41	0.30	DMF	100	10	54
18	Zr-guanine-MCM-41	0.30	DMSO	100	4	65
19	Zr-guanine-MCM-41	0.30	solvent-free	100	6	58
20	Zr-guanine-MCM-41	0.30	Dioxane	reflux	18	trace
21	Zr-guanine-MCM-41	0.30	acetonitrile	reflux	12	67
22	Zr-guanine-MCM-41	0.30	PEG-400	110	2	90
23	Zr-guanine-MCM-41	0.30	PEG-400	100	2	90
24	Zr-guanine-MCM-41	0.30	PEG-400	100	2	80
25	Zr-guanine-MCM-41	0.30	PEG-400	100	2	90
26	Zr-guanine-MCM-41	0.30	PEG-400	100	24	Trace

[a]Isolated yield.
[b]No reaction.

(Table 2, entry 11). No product was formed in the absence of the catalyst for 48 hr (Table 2, entry 5). Therefore, in order to find the best temperature, we investigated the reaction efficiency in various temperatures. Besides, it was noted that the temperature played an important role on the outcome of the reaction in the synthesis of 17-(4-chlorophenyl)-11*H*-benzo[*a*]benzo[6,7] chromeno[2,3-*c*]phenazine-11,16(17*H*)-dione. As a result, 100 °C was selected as the best temperature for this reaction (Table 2, entry 5).

After optimization of the reaction conditions, the scope of the catalyst was further explored and various aromatic aldehydes bearing electron-donating and electron-withdrawing substituents and isatin or ninhydrin as cyclic ketones were studied for One-pot, four-component domino synthesis of several benzo[*a*] benzo[6,7]chromeno[2,3-*c*]phenazine (Table 3, entries 1–10) and spiro[benzo[*a*]benzo[6,7]chromeno[2,3-*c*] phenazine] (Table 3, entries 11, 12) derivatives using a complex of Zr with 2-amino-1H-purin-6(9H)-one ligand supported into MCM-41 mesoporous. As it can be observed in Table 3, all aldehydes (containing electron-withdrawing and electron-donating groups) produced the desired derivative with good yields (Table 3). However, it is worth mentioning that in a fixed time interval, the aldehydes with electron-withdrawing groups show more reactivity than the aldehydes with electron-donating groups.

The mechanism for the synthesis of spiro[benzo[*a*] benzo[6,7]chromeno[2,3-*c*] phenazine] and benzo[*a*] benzo[6,7]chromeno[2,3-*c*]phenazine derivatives is proposed in Scheme 3. According to this mechanism, after

TABLE 3 One-pot multi-component domino synthesis of benzo[a]benzo[6,7]chromeno[2,3-c]phenazine (entries 1–10) and spiro[benzo[a]benzo[6,7]chromeno[2,3-c] phenazine] (entries 11, 12) derivatives using 25 mg Zr-guanine-MCM-41 as catalyst in PEG-400 at 100 °C for 2 hr

Entry	Product	Yield (%)[a]	M.p (°C)	
			Measured	Reported [Ref]
1	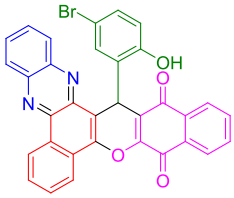	87	357–360[15]	359–361[41]
2	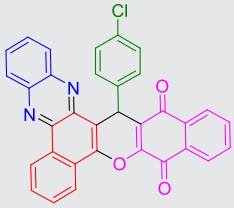	90	321–323	322–324[42]
3	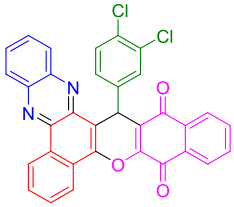	88	331–333[15]	330–332[41]
4	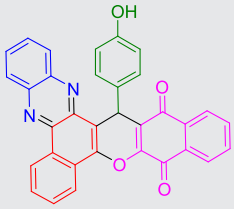	85	300–302[15]	301–332[42]
5	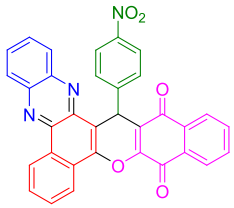	90	274–275[15]	270–272[42]
6		88	369–371	270–273[42]

TABLE 3 (Continued)

Entry	Product	Yield (%)[a]	M.p (°C)	
			Measured	Reported [Ref]
	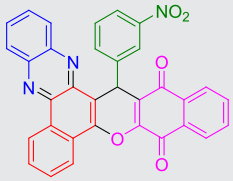			
7	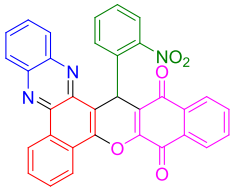	78	292–296	293–295[42]
8	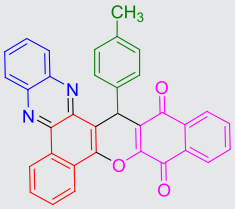	92	332–334[15]	330–333[42]
9	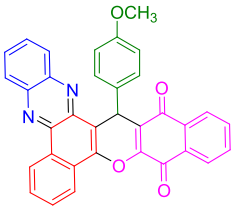	89	341–343[15]	340–342[42]
10	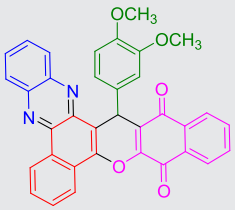	90	319–320[15]	320–321[43]
11		92	289–291	289–291[42]

(Continues)

TABLE 3 (Continued)

Entry	Product	Yield (%)[a]	M.p (°C)	
			Measured	Reported [Ref]
12	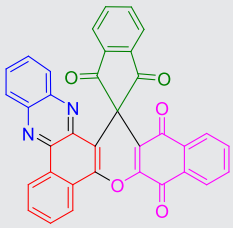	88	298–299[15]	297–299[43]
13	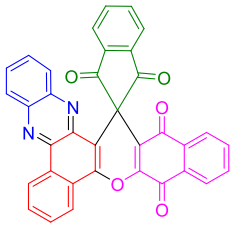	82	209–210[15]	210[43]

[a]Isolated yield.

tautomerization of 4-hydroxy-1,2-naphthoquinone (lawsone), the Schiff base reaction between 2-hydroxy-1,-4-naphthoquinone (1) and the benzene 1,2-diamine (2) in the presence of Zr-guanine-MCM-41 was performed in order to form the corresponding quinoxalinone A. Knoevenagel condensation of carbonyl groups of aldehydes with 4-hydroxy-1,2-naphthoquinone forming the olefin B. Finally, the Michael addition of the compound A with the compound B in the presence of the catalyst formed the intermediate C and, then, the inner molecular ring occurred to be formed after a tautomeric proton shift to generate spiro[benzo[*a*]benzo[6,7]chromeno[2,3-*c*] phenazine] and benzo[*a*]benzo[6,7]chromeno[2,3-*c*] phenazine derivatives.[5]

In the next part of this research project, the catalytic activity of Zr-guanine-MCM-41 for the synthesis of 4,4′-(arylmethylene)bis(3-methyl-1H-pyrazol-5-ols) was investigated. For this purpose, the condensation of *p*-Chlorobenzaldehyde (1 mmol) with, 3-Methyl-1-phenyl-5-pyrazolone (2 mmol) was selected as a model reaction to optimize the reaction conditions. Then, the effect of various parameters were studied; including, the amount of the catalyst, solvent and temperature on the reaction efficiency (Table 3). Initially, the effect of different amounts of the catalyst on the outcome of reaction was investigated. Among the various catalyst loadings (e.g., 0.05, 0. 1, 0.15, 0.20, 0.25 and 0.30 mol%), 0.25 mol% of the catalyst on the basis of Zr was selected as the most effective amount (Table 4, entry 6). Meanwhile, in the absence of the catalyst, the reaction didn't proceed at all even after 48 hr (Table 4, entry 5). Then, the influence of the solvent on the outcome of the reaction was studied. The obtained results revealed that ethanol is the most effective solvent for this type of domino reaction. Subsequently, the effect of temperature was examined, the results revealed that the highest yield of the product was obtained at 80 °C under reflux conditions. Eventually, EtOH at 80 °C in the presence of Zr-guanine-MCM-41 (0.25 mol%) was found to be the best choice for the mentioned model reaction.

SCHEME 3 One-pot, domino, multicomponent synthesis of benzo[a]benzo[6,7]chromeno[2,3-c]phenazine (b) and spiro[benzo[a]benzo[6,7]chromeno[2,3-c]phenazine] (c) derivatives in the presence of Zr-guanine-MCM-41

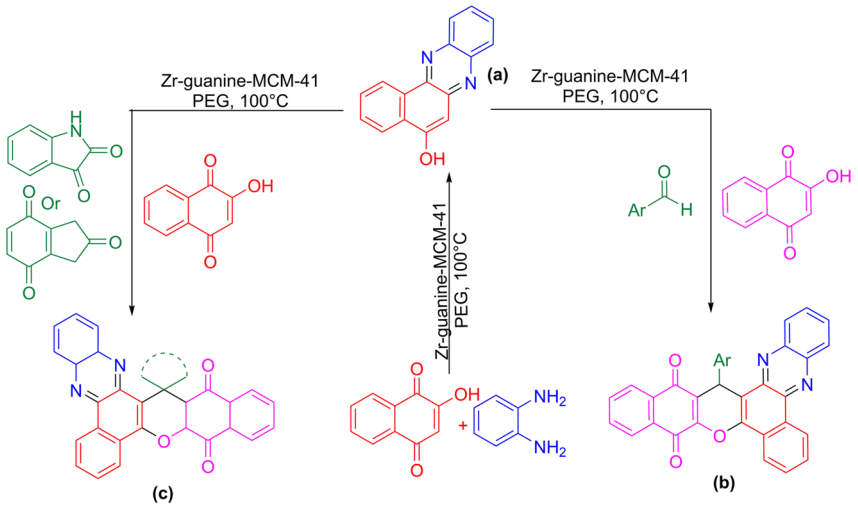

SCHEME 4 Proposed mechanism for the synthesis of benzo[a]benzo[6,7]chromeno[2,3-c]phenazine(E) and spiro[benzo[a]benzo[6,7]chromeno[2,3-c]phenazine] (D) derivatives

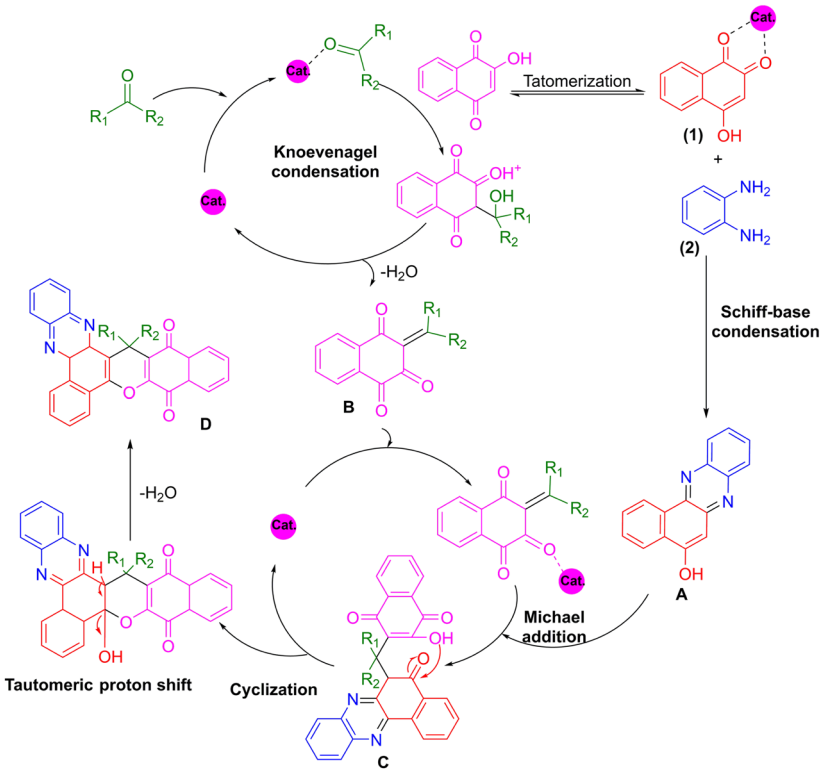

SCHEME 5 Optimization of reaction conditions for the synthesis of 4,4′-(arylmethylene)-bis-(3-methyl-1-phenyl-1H-pyrazol-5-ols)

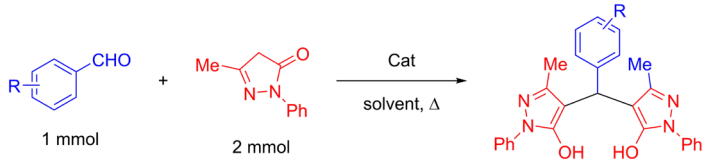

SCHEME 6 One-pot, domino, multicomponent synthesis of 4,4′-(arylmethylene)-bis-(3-methyl-1-phenyl-1H-pyrazol-5-ols) in the presence of Zr-guanine-MCM-41

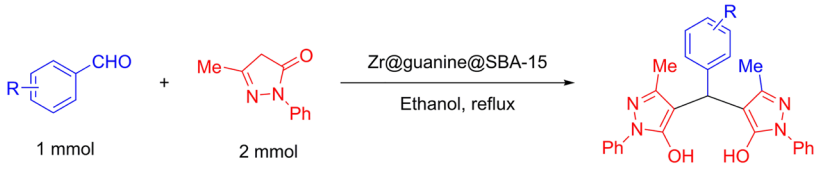

TABLE 4 Screening of the reaction parameters for the synthesis of 4,4′-(arylmethylene)-bis-(3-methyl-1-phenyl-1H-pyrazol-5-ols)

Entry	Catalyst	Amount of Catalyst (mol%)	Solvent	Temperature (°C)	Time (min)	Yield (%)[a]
1	$ZrO\ Cl_2.8H_2O$	0.25	EtOH	Reflux	48 h	Trace
2	guanine	0.25	EtOH	Reflux	48 h	NR[b]
3	MCM-41	25 mg	EtOH	Reflux	48 h	NR[b]
4	Zr-MCM-41	25 mg	EtOH	Reflux	2 h	63
5	guanine-MCM-41	25 mg	EtOH	Reflux	48 h	NR[b]
6	-	-	EtOH	Reflux	48 h	NR[b]
7	Zr-guanine-MCM-41	0.05	EtOH	Reflux	15	39
8	Zr-guanine-MCM-41	0.10	EtOH	Reflux	15	67
9	Zr-guanine-MCM-41	0.15	EtOH	Reflux	15	83
10	Zr-guanine-MCM-41	0.20	EtOH	Reflux	15	91
11	Zr-guanine-MCM-41	0.25	EtOH	Reflux	15	98
12	Zr-guanine-MCM-41	0.30	EtOH	Reflux	15	98
13	Zr-guanine-MCM-41	0.25	Acetonitrile	80	15	83
14	Zr-guanine-MCM-41	0.25	PEG-400	80	15	80
15	Zr-guanine-MCM-41	0.25	acetone	Reflux	15	53
16	Zr-guanine-MCM-41	0.25	*n*-Hexane	Reflux	15	Trace
17	Zr-guanine-MCM-41	0.25	DMF	80	15	63
18	Zr-guanine-MCM-41	0.25	DMSO	80	15	72
19	Zr-guanine-MCM-41	0.25	Dioxane	Reflux	15	38
20	Zr-guanine-MCM-41	0.25	H_2O	80	15	63
21	Zr-guanine-MCM-41	0.25	solvent-free	80	15	Trace
22	Zr-guanine-MCM-41	0.25	acetonitrile	25	15	10
23	Zr-guanine-MCM-41	0.25	acetonitrile	70	15	75
24	Zr-guanine-MCM-41	0.25	EtOH	25	15	NR[b]
25	Zr-guanine-MCM-41	0.25	EtOH	40	15	37
26	Zr-guanine-MCM-41	0.25	EtOH	50	15	59
27	Zr-guanine-MCM-41	0.25	EtOH	60	15	79
28	Zr-guanine-MCM-41	0.25	EtOH	65	15	87
29	Zr-guanine-MCM-41	0.25	EtOH	70	15	91

[a]Isolated yield.
[b]No reaction.

In order to investigate the scope and generality of this procedure, different electron-withdrawing or electron-donating groups, such as OCH_3, NO_2, and CH_3, were selected to react 3-Methyl-1-phenyl-5-pyrazolone under the optimized reaction conditions. The results are summarized in Table 5. The experimental results show that various aromatic aldehydes having both electron-withdrawing and electron-donating groups (such as Cl, Br, OH, OCH_3, NO_2, and CH_3) produced their corresponding derivatives in good to excellent yields. However, it is worth mentioning that the reaction time of the aryl aldehydes with electron-donating groups on the aromatic ring was longer than aryl aldehydes with electron-withdrawing groups. In order to show the chemoselectivity of this new catalytic system, the reaction of terephthaldehyde was also investigated in which the NMR investigations show that, both of the aldehyde Substituents on aromatic ring showed good reactivity and the corresponding 4′,4″,4‴-(1,4-Phenylenebis (methanetriyl))tetrakis (3-methyl-1-phenyl-1H-pyrazol-5-ol) product was obtained in 83% yield (Tables 5 entry 10).

The suggested reaction mechanism for the described combination via tandem Knoevenagel–Michael reaction in the presence of Zr-guanine-MCM-41 nanocatalyst has been depicted in Scheme 7 based on the previously reported reaction pathway.[51] Initially, intermediate **III** formed from the Knoevenagel condensation of aldehyde and Pyrazolone in the presence of Zr-guanine-MCM-41

TABLE 5 Preparation of 4,4′-(arylmethylene)-bis-(3-methyl-1-phenyl-1H-pyrazol-5-ols) derivatives catalyzed by Zr-guanine-MCM-41

Entry	Product	Time (min)	Yield (%)[a]	M.P. (°C)	
				Measured	Reported [Ref]
1	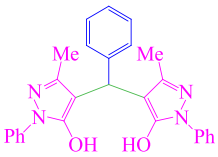	20	99	170–173	170–172[20]
2	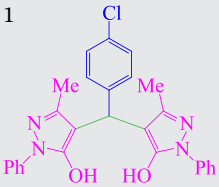	15	98	212–214	213–215[11]
3	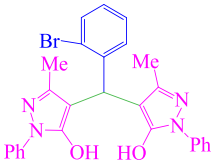	10	98	198–200	198–200[19]
4	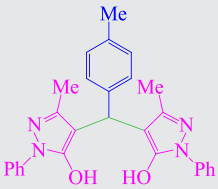	25	97	201–203	202–204[20]
5	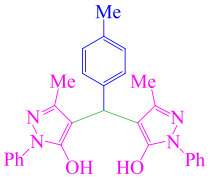	30	90	173–175	173–175[11]
6	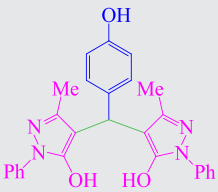	25	88	153–155	153–155[11]
7		45	95	195–197	194–196[11]

(Continues)

TABLE 5 (Continued)

Entry	Product	Time (min)	Yield (%)[a]	M.P. (°C)	
				Measured	Reported [Ref]
	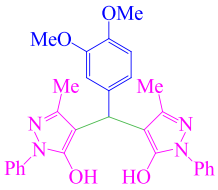				
8	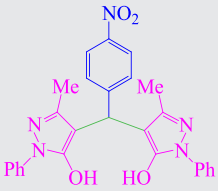	10	92	224–226	225–227[19]
9	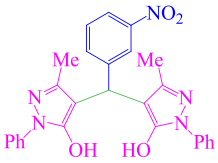	15	91	150–152	151–153[12]
10	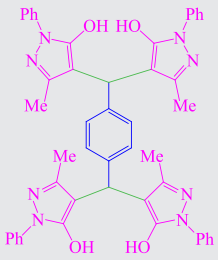	60	83	214–216	214–216[19]

[a]Isolated yield.

nanocatalyst. Sequentially, a possible intermediate **IV** was formed via Michael addition of the second mol of Pyrazolone with intermediate **III** to give bis (pyrazolyl) methanes.

3.4 | Catalyst reusability

The reusability of the catalyst is an important benefit especially for industrial and commercial applications. Thus, the recovery and reusability of the nanocatalyst were investigated in the synthesis of 17-(4-chlorophenyl)-11*H*-benzo[*a*]benzo[6,7]chromeno[2,3-*c*]phenazine-11,16(17*H*)-dione and 4,4′-((4-chlorophenyl)methylene) bis(3-methyl-1-phenyl-1H-pyrazol-5-ol) under the optimized reaction conditions (the amount of the reactants and catalyst was tripled). After completion of the reaction, the chemicals were placed in a separatory funnel and, then, separated into an organic and aqueous layer. The catalyst was separated by simple filtration, washed with hot EtOH and acetone to remove the residual product and reused in the subsequent runs. This result showed that the catalyst is robust and has fine running cycling performance (Figure 10).

SCHEME 7 Proposed mechanism for the synthesis of 4,4′-(arylmethylene)-bis-(3-methyl-1-phenyl-1H-pyrazol-5-ols)

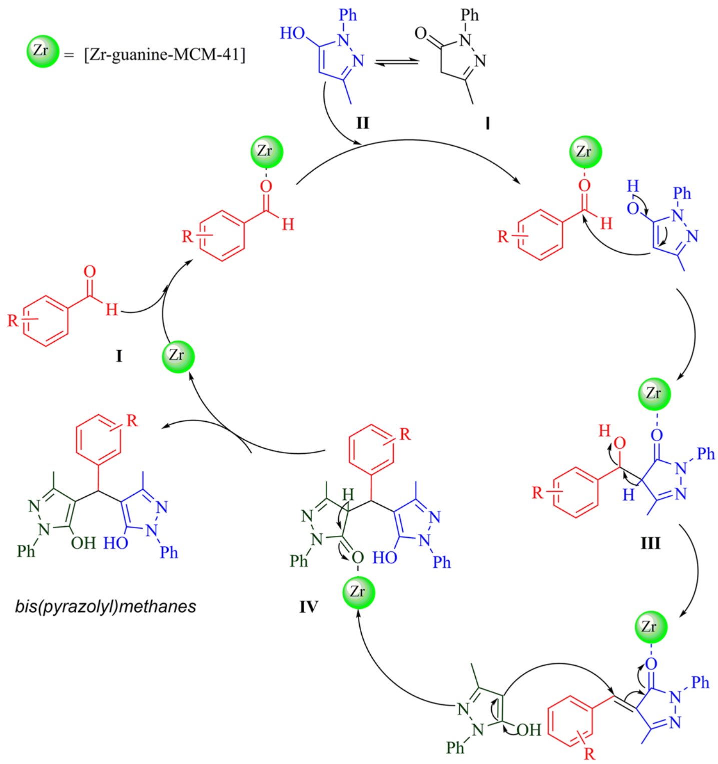

Moreover, in order to examine the stability of the catalyst after the recycling, the recycled catalyst has been characterized by SEM, TEM and FT-IR techniques. These characterizations confirmed that the recovered catalyst is in good agreement with the fresh catalyst. These characterizations are strong evidences for the high stability of Zr-guanine-MCM-41 after recycling.

The SEM image of the recycled catalyst is shown in Figure 11 in which particles of the recovered catalyst were observed between 15–20 nm with homogeneous size and morphology. In addition, The SEM image also showed some evidences of slight aggregation and fusing.

FT-IR spectrums of the recycled catalyst are shown in Figure 12. The results show that a good agreement was observed for FT-IR of the fresh Zr-guanine-MCM-41 (Figure 12a) and the recycled catalyst (Figure 12b). Therefore, Figure 12 illustrates the good stability of Zr-guanine-MCM-41 after recycling.

3.5 | Hot filtration test

Moreover, hot filtration test was performed in order to prove that the metal was not leaching out from the solid catalyst during the reactions. For this purpose, the reaction of 2-hydroxy-1,4-naphthoquinone (1 mmol) and the benzene 1,2-diamine (1 mmol) in the presence of Zr-guanine-MCM-41 (25 mg) was performed in the first step and the condensation between 2-hydroxy-1,-4-naphthoquinone (1 mmol) with 4-chlorobenzaldehyde (1 mmol) in the second step in PEG-400 at 100 °C. When about 50% of the reaction was done, the catalyst was

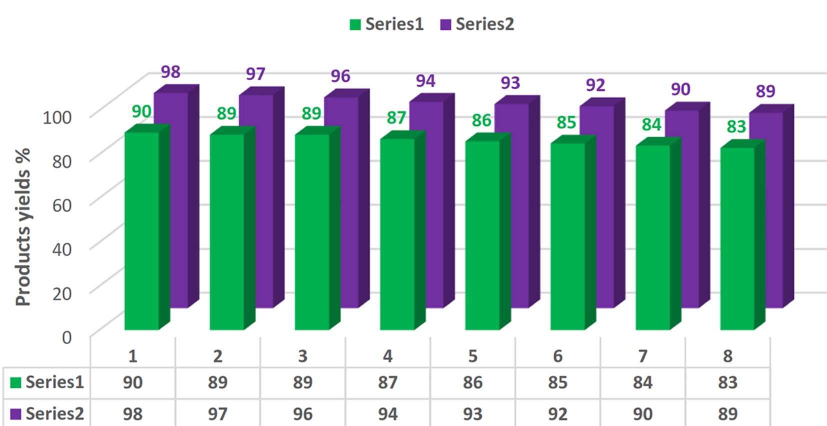

FIGURE 10 Reusability of Zr-guanine-MCM-41 nanocatalyst for the synthesis of 17-(4-chlorophenyl)-11H-benzo[a]benzo[6,7]chromeno[2,3-c]phenazine-11,16(17H)-dione (series 1) and 4,4′-((4-chlorophenyl)methylene)bis(3-methyl-1-phenyl-1H-pyrazol-5-ol) (series 2) reactions

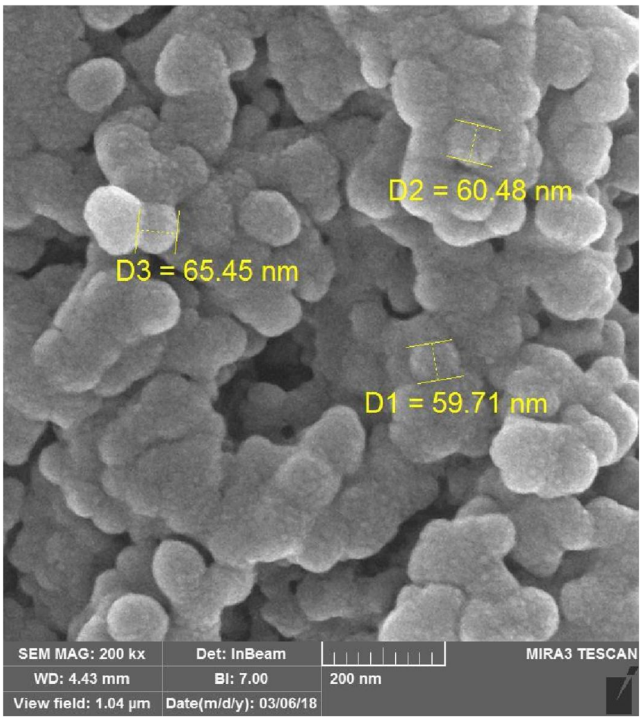

FIGURE 11 SEM image of recycled Zr-guanine-MCM-41

filtered off at the reaction temperature and the experiment was continued without the catalyst for another half reaction time. The observation indicated that there was no detectable progress in the reaction.

3.6 | Leaching test

In order to consider the leaching of Zr into reaction media, ICP-AES analysis was performed, the Zirconium content in reaction media in the synthesis of 17-(4-chlorophenyl)-11H-benzo[a]benzo[6,7]chromeno[2,3-c]phenazine-11,16(17H)-dione and 4,4′-((4-chlorophenyl)methylene)bis(3-methyl-1-phenyl-1H-pyrazol-5-ol) was found to be 0.39 and 0.47% respectively. The results show that the leaching of Zr into reaction media is negligible.

3.7 | Comparison

The efficiency of this catalytic system was demonstrated by comparing our results on the synthesis of

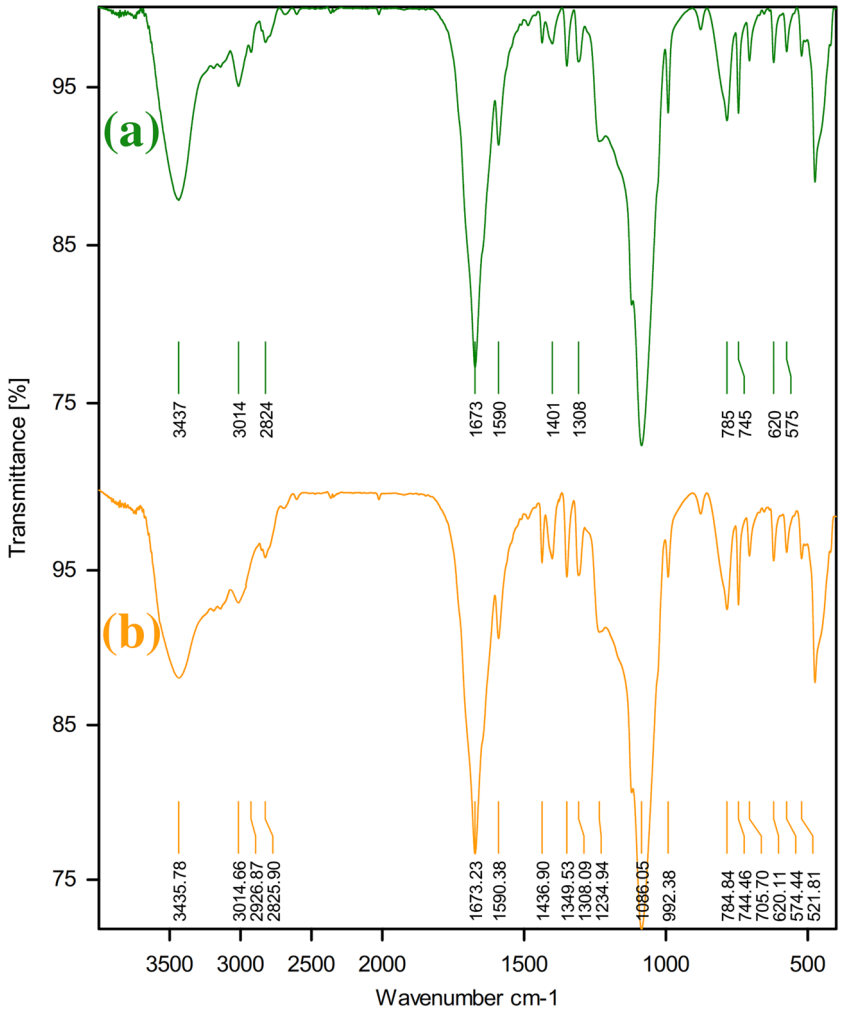

FIGURE 12 FT-IR spectrums of Zr-guanine-MCM-41(a) and recovered Zr-guanine-MCM-41

TABLE 6 Comparison of Zr-guanine-MCM-41for the synthesis of 17-(4-Methyl)-11H–benzo[a]benzo[6,7]chromeno[2,3-c] phenazine-11,16 (17H)-dione and 4,4′-((4-chlorophenyl)methylene)bis(3-methyl-1-phenyl-1H-pyrazol-5-ol) with previously reported procedures

Entry	Substrate	Catalyst	Catalyst nature	Time (min)	Yield (%)[a]	Ref
1	4-$CH_3C_6H_4$	p-toluenesulfonic acid	Homogeneous	120	87	[46]
2	4-$CH_3C_6H_4$	Ni-Gly-isatin@boehmite	Heterogeneous	420	80	[47]
3	4-$CH_3C_6H_4$	γ-Fe_2O_3@SiO_2-SCH_2CO_2H	Heterogeneous	180	89	[15]
4	4-$CH_3C_6H_4$	Zr-guanine-MCM-41	Heterogeneous	120	92	This work
5	4-Cl C_6H_4	Na^+-MMT-[pmim]HSO_4	Heterogeneous	10	92	[52]
6	4-Cl C_6H_4	Nanocrystalline Cu–ZnO	Heterogeneous	90	93	[53]
7	4-Cl C_6H_4	$CuFe_2O_4$ MNPs	Heterogeneous	15	89	[54]
8	4-Cl C_6H_4	Zr-guanine-MCM-41	Heterogeneous	15	98	This work

[a]Isolated yield.

17-(4-Methyl)-11H–benzo[a]benzo[6,7]chromeno[2,3-c] phenazine-11,16 (17H)-dione (Table 6 entry 1–4) and 4,4′-((4-chlorophenyl)methylene)bis(3-methyl-1-phenyl-1H-pyrazol-5-ol) with some recent reported catalytic systems in the literatures (Table 6 entry 5–8). The summarized results in Table 6 obviously show that the present protocol provides better results in terms of the reaction time and product yield. Besides, this catalyst is comparable in terms of price, non-toxicity, stability and easy separation.

4 | CONCLUSIONS

Finally, we have introduced an efficient Zr-guanine-MCM-41 catalyzed, one-pot multicomponent tandem Knoevenagel condensation–Michael addition–cyclization reactions for the selective synthesis of benzo[*a*]benzo[6,7] chromeno[2,3-*c*]phenazine, spiro[benzo[*a*]benzo[6,7] chromeno[2,3-*c*] phenazine] and Bis (pyrazolyl)methane derivatives (which could be of biological significance) under green conditions. The catalyst was prepared by the immobilization of Zr@2-amino-1H-purin-6(9H)-one supported into MCM-41 mesoporous (Zr-guanine-MCM-41) by covalent cross-linking. The structure of the prepared Zr nanocatalyst was characterized by FT-IR, Raman, XRD, BET, TGA, EDX, ICP, AAS, X-Ray mapping, SEM and TEM techniques. The product required a minimum of time, cost, labor, and waste production and was obtained in good to excellent yields. High-yielding of the products in pure form was the fundamental characteristic of this protocol. Operational simplicity, ease of the catalyst recovery and its good performance under mild reaction conditions are the other advantages of this methodology. Furthermore, catalytic activity of Zr-guanine-MCM-41catalyst was compared to the previously reported ones. Additionally, the Zr-guanine-MCM-41 is more economic and environment friendly because of its low Zr leaching. This recoverable catalyst, Zr (IV) oxide chloride, has been synthesized and characterized using TGA, XRD, BET, ICP, AAS, SEM, TEM, Raman, EDX and FT-IR spectroscopy. Moreover, the recovery test confirms that the synthesized catalyst can be reused for several times. In addition, the recovered catalyst was characterized by SEM and FT-IR techniques.

ACKNOWLEDGMENTS

This work was supported by the Iran National Science Foundation and research facilities of Ilam University, Ilam, Iran.

ORCID

Mohsen Nikoorazm https://orcid.org/0000-0002-4013-0868

Masoud Mohammadi https://orcid.org/0000-0002-1043-3470

REFERENCES

[1] S. Mahmoudi-GomYek, D. Azarifar, M. Ghaemi, H. Keypour, M. Mahmoudabadi, *Appl. Organomet. Chem.* **2019**, *33*, e4918.
[2] M. Daraie, M. M. Heravi, M. Mirzaei, N. Lotfian, *Appl. Organomet. Chem.* **2019**, *33*, e5058.
[3] S. Shojaei, Z. Ghasemi, A. Shahrisa, *Appl. Organomet. Chem.* **2017**, *31*, e3788.
[4] M. Kazemi, M. Mohammadi, *Appl. Organomet. Chem.* **2020**, *34*, e5400.
[5] A. Ghorbani-Choghamarani, M. Mohammadi, R. H. E. Hudson, T. Tamoradi, *Appl. Organomet. Chem.* **2019**, *33*, e4977.
[6] S. R. Mousavi, H. Sereshti, H. Rashidi Nodeh, A. Foroumadi, *Appl. Organomet. Chem.* **2019**, *33*.
[7] M. Neysi, A. Zarnegaryan, D. Elhamifar, *New J. Chem.* **2019**, *43*, 12283.
[8] M. Nikoorazm, M. Khanmoradi, M. Mohammadi, *Appl. Organomet. Chem.* **2020**, e5504.

[9] A. Ghorbani-Choghamarani, M. Mohammadi, T. Tamoradi, M. Ghadermazi, *Polyhedron* **2019**, *158*, 25.
[10] L. Wang, Y. B. Xie, Q. L. Yang, M. G. Liu, K. B. Zheng, H. Y. Lin, N. Y. Huang, *J. Iran. Chem. Soc* **2016**, *13*, 1797.
[11] T. Tamoradi, S. M. Mousavi, M. Mohammadi, *New J. Chem.* **2020**, *44*, 3012.
[12] Y. Y. Titova, F. K. Schmidt, *Catal. Letters* **2018**, *148*, 2719.
[13] M. Glavaš, M. Gredičak, I. Jerić, *ACS Comb. Sci.* **2018**, *20*, 151.
[14] X. Fang, Z. Deng, W. Zheng, J. C. Antilla, *ACS Catal.* **2019**, *9*, 1748.
[15] M. Vilches-Herrera, L. Domke, A. Börner, *ACS Catal.* **2014**, *4*, 1706.
[16] R. Marín-Valls, K. Hernández, M. Bolte, J. Joglar, J. Bujons, P. Clapés, *ACS Catal.* **2019**, *9*, 7568.
[17] A. Dömling, W. Wang, K. Wang, *Chem. Rev.* **2012**, *112*, 3083.
[18] A. Chaudhary, J. M. Khurana, *Res. Chem. Intermed.* **2018**, *44*, 1045.
[19] A. Ghorbani-Choghamarani, M. Mohammadi, L. Shiri, Z. Taherinia, *Res. Chem. Intermed.* **2019**, *45*, 5705.
[20] N. Guttenberger, W. Blankenfeldt, R. Breinbauer, *Bioorganic Med. Chem.* **2017**, *25*, 6149.
[21] M. Norouzi, D. Elhamifar, *Catal. Letters* **2019**, *149*, 619.
[22] M. A. Zolfigol, A. Khazaei, F. Karimitabar, M. Hamidi, *Appl. Sci.* **2016**, *6*, 1.
[23] M. Shekouhy, R. Kordnezhadian, A. Khalafi-Nezhad, *J. Iran. Chem. Soc.* **2018**, *15*, 2357.
[24] S. Farhadi, K. Jahanara, A. Sepahdar, *J. Iran. Chem. Soc.* **2014**, *11*, 1103.
[25] D. Azarifar, S. M. Khatami, M. A. Zolfigol, R. Nejat-Yami, *J. Iran. Chem. Soc.* **2014**, *11*, 1223.
[26] A. Hasaninejad, M. Shekouhy, A. Zare, S. M. S. Hoseini Ghattali, N. Golzar, *J. Iran. Chem. Soc.* **2011**, *8*, 411.
[27] K. Niknam, S. Mirzaee, *Synth. Commun.* **2011**, *41*, 2403.
[28] N. I. Vazquez, Z. Gonzalez, B. Ferrari, Y. Castro, *Bol. La Soc. Esp. Ceram. Y Vidr.* **2017**, *56*, 139.
[29] Q. Pu, M. Kazemi, M. Mohammadi, *Mini. Rev. Org. Chem.* **2019**, *16*, 5775.
[30] M. Kazemi, S. M. Nasr, Z. Chen, M. Mohammadi, *Mini. Rev. Org. Chem.* **2019**, *16*, 1.
[31] L. Chen, A. Noory Fajer, Z. Yessimbekov, M. Kazemi, M. Mohammadi, *J. Sulfur Chem.* **2019**, *40*, 451.
[32] M. Mohammadi, A. Ghorbani-Choghamarani, *New J. Chem.* **2020**, *44*, 2919.
[33] M. Hami Dindar, M. R. Yaftian, M. Pilehvari, S. Rostamnia, *J. Iran. Chem. Soc.* **2015**, *12*, 561.
[34] M. Eslami, M. G. Dekamin, L. Motlagh, A. Maleki, *Green Chem. Lett. Rev.* **2018**, *11*, 36.
[35] A. Mehmood, H. Ghafar, S. Yaqoob, U. F. Gohar, B. Ahmad, *J. Dev. Drugs* **2017**, *06*.
[36] N. Bahri-Laleh, S. Sadjadi, M. M. Heravi, M. Malmir, *Appl. Organomet. Chem.* **2018**, *32*.
[37] D. Gopalakrishnan, S. Srinath, B. Baskar, N. S. P. Bhuvanesh, M. Ganeshpandian, *Appl. Organomet. Chem.* **2019**, *33*.
[38] A. Ghorbani-Choghamarani, M. Mohammadi, Z. Taherinia, *Chem. Soc.* **2019**, *16*, 411.
[39] M. Khanmoradi, M. Nikoorazm, A. Ghorbani-Choghamarani, *Catal. Letters* **2017**, *147*, 1114.
[40] H. Filian, A. Ghorbani-Choghamarani, E. Tahanpesar, *J. Porous Mater.* **2019**, *26*, 1091.
[41] R. Mohebat, A. Yazdani Elah Abadi, M. T. Maghsoodlou, M. Mohammadi, *Res. Chem. Intermed.* **2016**, *42*, 5915.
[42] A. Ghorbani-Choghamarani, R. Sahraei, Z. Taherinia, *Res. Chem. Intermed.* **2019**, *45*, 3199.
[43] S. Abbasi Pour, A. Yazdani-Elah-Abadi, M. Afradi, *Appl. Organomet. Chem.* **2017**, *31*, e3791.
[44] K. Guo, F. Han, Z. Arslan, J. McComb, X. Mao, R. Zhang, S. Sudarson, H. Yu, *Water, Air, Soil Pollut.* **2015**, *226*, 288.
[45] M. Nikoorazm, A. Ghorbani-Choghamaranai, M. Khanmoradi, P. Moradi, *J. Porous Mater.* **2018**, *25*, 1831.
[46] M. Nikoorazm, A. Ghorbani-Choghamarani, M. Khanmoradi, **2016**, *6*, 56549.
[47] M. Nikoorazm, A. Ghorbani-Choghamarani, M. Khanmoradi, *J. Porous Mater.* **2016**, *23*, 761.
[48] M. Nikoorazm, A. Ghorbani-Choghamarani, M. Khanmoradi, *J. Iran. Chem. Soc.* **2017**, *14*, 1215.
[49] T. Tamoradi, A. Ghorbani-Choghamarani, M. Ghadermazi, *Appl. Organomet. Chem.* **2018**, *32*, e4340.
[50] S. Molaei, T. Tamoradi, M. Ghadermazi, A. Ghorbani-Choghamarani, *Microporous Mesoporous Mater.* **2018**, *272*, 241.
[51] S. Sobhani, A. R. Hasaninejad, M. F. Maleki, Z. P. Parizi, *Synth. Commun.* **2012**, *42*, 2245.
[52] F. Shirini, M. Seddighi, M. Mazloumi, M. Makhsous, M. Abedini, *J. Mol. Liq.* **2015**, *208*, 291.
[53] S. Shinde, B. Karale, D. Bankar, S. Arbuj, M. Moulavi, D. Amalnerkar, T. Kim, *J. Nanosci. Nanotechnol.* **2019**, *19*, 4623.
[54] R. Khalifeh, R. Shahimoridi, M. Rajabzadeh, *Catal. Letters* **2019**, *149*, 2864.

How to cite this article: Nikoorazm M, Mohammadi M, Khanmoradi M. Zirconium@guanine@MCM-41 nanoparticles: An efficient heterogeneous mesoporous nanocatalyst for one-pot, multi-component tandem Knoevenagel condensation–Michael addition–cyclization Reactions. *Appl Organomet Chem*. 2020; e5704. https://doi.org/10.1002/aoc.5704